

Electrical Structure of PbS Films*

D. P. SNOWDEN† AND A. M. PORTIS

Department of Physics, University of California, Berkeley, California

(Received April 18, 1960; revised manuscript received September 2, 1960)

The electrical properties of chemically deposited lead sulfide films have been investigated as a function of frequency from dc into the microwave range. Conductivity and Hall mobility measurements have been made on both the dark and the photoexcited carriers. The dark conductivity is independent of frequency below 100 Mc/sec. It increases by almost an order of magnitude over a decade in frequency and then becomes constant again at higher frequencies. This behavior is typical of a material whose low-frequency conductivity is limited by barriers. Surprisingly the photoconductivity behaves quite differently. The photoconductivity has a hump around 100 Mc/sec but otherwise is relatively independent of frequency. The Hall mobilities of the dark and photocarriers are equal at dc in agreement with earlier studies. Microwave Hall measurements indicate that the dark carriers have about the same apparent mobility at 10 kMc/sec as at dc. It is shown that the conventional barrier model with a photoinduced

change in carrier concentration cannot account for the behavior of these films. Nor can a model in which the barrier height is modified by illumination. The present studies suggest that there are connecting channels through the films and that the photoresponse of the films is determined by the behavior of these channels. A simple model is constructed and its parameters are adjusted to fit the conductivity data and the dc Hall mobility. As a check on the model the measured microwave Hall mobility is compared with the predicted value. Good agreement is found for high-quality commercial films. The hump observed in the photoconductivity follows naturally from this model, being associated with a modulation of the barrier capacitance. Studies of the photoconductive decay yield the same time constant at dc and microwave frequencies, supporting the picture that the same photocarriers are responsible for the dc and microwave photoconductivity.

I. INTRODUCTION

FILMS of the lead salts are of considerable interest in that they provide the fastest and most sensitive detectors known for near infrared radiation. Although there has been considerable experimental and theoretical work on these films over the past ten years,¹ the mechanism of photoconduction in the lead salt films is still not firmly established. This paper reports on radio- and microwave-frequency studies of the dark conductivity, photoconductivity, and dark and photomobility of chemically deposited PbS films.²

This study was stimulated by the development in this laboratory of a technique for making precise measurements of carrier mobilities at microwave frequencies.³ We hoped that this technique might provide a useful tool for the study of lead salt films because of the general opinion that these films were composed of small regions of reasonably high carrier mobility, separated by barriers. Two fundamentally different mechanisms had been proposed to account for the photoconductivity of these films. One model treated the barrier as a thin

insulating region over which the carriers might be thermally excited.⁴ On this model the carrier concentration in the conducting region is increased by illumination and the increase in conductivity of the films is simply proportional to the change in carrier concentration. A second model calls attention to the barrier region.⁵ It is pointed out that the space charge near the barrier will be modified by illumination and that the barrier height will be altered. Since the film conductivity is extremely sensitive to barrier height, it might be expected that a photoinduced change in the barrier height could be the dominant mechanism of photoconductivity. Convincing arguments have been made for both models without any clear basis for choice. It was hoped that microwave mobility measurements supported by an extensive study of dark and photoconductivity as a function of electrical frequency would yield conclusive structural information about these films, which would resolve the controversy.

As is demonstrated in Sec. II, the dark conductivity of the films as a function of frequency establishes that the dc conductivity is limited by barriers in agreement with both the numbers modulation model and the barrier modulation model. The conductivity is observed to increase by nearly an order of magnitude over a decade in frequency, being independent of frequency both below and above the transition region. This behavior establishes that there are two well-defined regions within the films.

In Sec. III the measurement of photoconductivity as a function of frequency is discussed. The photocon-

* This work was supported by the U. S. Atomic Energy Commission.

† Now at John J. Hopkins Laboratory for Pure and Applied Science, General Atomic Division of General Dynamics, San Diego, California.

¹ See the review papers of R. A. Smith, *Advances in Physics*, edited by N. F. Mott (Taylor and Francis, Ltd., London, 1953), Vol. 2, p. 321; and F. S. Moss, *Proc. Inst. Radio Engrs.* **43**, 1869 (1955).

² We are grateful to Dr. H. E. Spencer of the Eastman-Kodak company for making available a number of extremely high quality PbS films. Dr. R. F. Brebrick of the U. S. Naval Ordnance Laboratory, White Oak, very kindly made available a large number of experimental films of widely varying characteristics. A preliminary account of this work has been given by D. P. Snowden, A. M. Portis, and R. F. Brebrick, *Bull. Am. Phys. Soc.* **3**, 410 (1958). The authors wish to withdraw some of the opinions expressed in this abstract.

³ A. M. Portis and D. T. Teaney, *J. Appl. Phys.* **29**, 1692 (1958); A. M. Portis *J. Phys. Chem. Solids* **8**, 326 (1959).

⁴ Richard L. Petritz, *Phys. Rev.* **104**, 1508 (1956).

⁵ A. F. Gibson, *Proc. Roy. Soc. (London)* **B64**, 603 (1951); G. W. Mahlman, W. B. Nottingham, and J. C. Slater, *Proceedings of the Conference on Photoconductivity, Atlantic City, November 4-6, 1954*, edited by R. G. Breckenridge *et al.* (John Wiley & Sons, New York, 1956); J. C. Slater, *Phys. Rev.* **103**, 1631 (1956).

ductivity goes through a maximum in the transition region dropping at high frequencies to a value comparable to the low-frequency value. Unfortunately, this kind of behavior is expected on neither the numbers or barrier modulation model. Clearly, on the numbers model the responsivity, which is the ratio of the change in conductivity with illumination to the dark conductivity, should be independent of frequency, and should be simply equal to the fractional increase in carrier concentration. On the other hand, the barrier modulation model yields a responsivity which decreases monotonically with frequency as the capacitance shunting the barrier reduces its impedance. In the limit of high frequencies the responsivity should approach zero on the latter model.

In Sec. IV we describe the dc Hall mobility measurements. Our results are in good agreement with earlier studies of Woods⁶ yielding mobilities of the order of $10 \text{ cm}^2/\text{volt-sec}$ for these films and establishing that the mobilities of the dark and photocarriers as measured at dc are equal. Woods, on this basis of his studies, found evidence for the numbers modulation model. He argued that if the dominant effect of illumination were to reduce the barrier height this could be regarded as an effective increase in carrier mobility and the apparent Hall mobility of the photocarriers would then be twice the apparent Hall mobility of the dark carriers. Since no difference in the two mobilities can be measured, Woods concludes that the light does not appreciably alter the carrier mobilities but can only change their number. We are in agreement with this conclusion of Woods although we cannot agree that these measurements establish the validity of the numbers modulation model.

On the basis of the observed increase in dark conductivity by a factor of ten, one might expect that the apparent carrier mobilities measured at microwave frequencies would be an order of magnitude higher than the dc mobilities. This would be the case if the dc mobility were barrier-limited. As is discussed in Sec. V, the microwave mobility is of the order of magnitude of the dc mobility in value. These measurements force us to the conclusion that the dc mobility is not barrier-limited. We must conclude that mobilities of the order of $10 \text{ cm}^2/\text{volt-sec}$ represent true bulk mobilities within the films and that the dc current is carried through the film by connecting channels, which are in shunt with the barrier regions. The dc data taken alone, might then lead to the conclusion that the barriers are partially shorted but that in other respects the numbers model describes the effect of illumination. Such a picture will not give the observed frequency dependence of the photoconductivity. Any model which excites carriers uniformly through the film must give a responsivity independent of frequency. But the fact that the absolute change in conductivity measured at dc and at microwave frequencies is about the same suggests instead

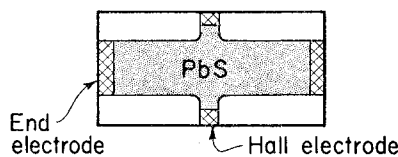
that the photoconducting channels not only shunt the barriers but also shunt the isolated regions themselves.

A simplified film structure which incorporates these ideas is described in Sec. VI. By assuming that the conductivity increase is restricted to the channels, there are a sufficient number of parameters available so that we can fit the dark and photoconductivity and the dc Hall mobility. These data uniquely fix the parameters in the model. The frequency dependence of the photoconductivity follows naturally from this model with the hump in the photoconductivity being associated with a reduction in barrier reactance with photoexcitation.

In Sec. VII we compare our calculations with the experimental measurements. We find that the experimental values and the predicted values are in good agreement for the high sensitivity E-K films which we have examined. We do not obtain agreement for the low-sensitivity experimental films. We are uncertain about the source of the discrepancy in the latter case although our model in restricting the increase in conductivity to the channels may be overly restrictive for the low-sensitivity films. One could presumably achieve agreement by relaxing this restriction, but we have not attempted to do this since our main interest has been in obtaining a description of the high-sensitivity films.

In Sec. VIII we discuss briefly the physical basis of film behavior as suggested by these experiments. We find in agreement with other investigators that the exceptional sensitivity of these films is because of the achievement of extremely long photocarrier lifetimes in the connected paths. We have measured decay times for the photocarriers and find them as long as 560 microseconds in the most sensitive films. The microwave current and the dc current decay with the same characteristic time, confirming that the same carriers are responsible for the current increase at both frequencies. Finally, some evidence from film spot scanning studies is presented to support the idea that the films as a whole

(a)



(b)

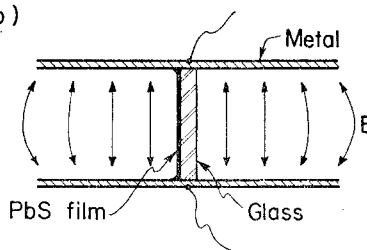


FIG. 1. (a) Typical PbS film as prepared for dc conductivity and Hall measurements. The method shown eliminates the introduction of noise from the Hall electrodes. (b) A film as prepared for radio-frequency conductivity measurements. The parallel end plates insure that the electric field is parallel to the sample surface.

⁶ Joseph H. Woods, Phys. Rev. **106**, 235 (1957).

are not activated, but only the channels which form a small fraction of the film.

II. DARK CONDUCTIVITY

There have been a number of studies of the frequency dependence of electrical conductivity in lead salt films up to frequencies in the microwave region.⁷ However, as Broudy and Levinstein⁸ have shown, these early results were dominated by gross nonuniformities in the film structure. With the development of much more uniform films a much weaker and more gradual increase in conductivity with frequency is observed. Rittner and Grace⁹ have suggested that this increase is not an intrinsic bulk property of the films but is instead a self-capacitance effect. This point of view has been fully supported by the theoretical work of Lax and Sachs¹⁰ who have used a variational method to calculate the frequency dependence of the film conductivity. Recently, it has been possible to separate bulk and capacitance effects for a few selected films¹¹ using this theory.

It seemed to us that rather than make measurements using conventional end electrodes of the kind shown in Fig. 1(a), and attempt to separate out the intrinsic frequency effect analytically, we might consider a modification in the electrodes. By making the electrodes in the form of parallel plates as shown in Fig. 1(b), the electric field is forced to remain parallel to the film surface. Under these conditions there is no formation of surface charge and no development of the complex field configurations which require special analytical treatment. With the geometry which we have used the film conductance and the susceptance of the capacitor are in parallel and simply add. In Fig. 2 the conductance of a film with conventional end electrodes and with parallel plates are compared from 50 kc/sec to 50 Mc/sec. The

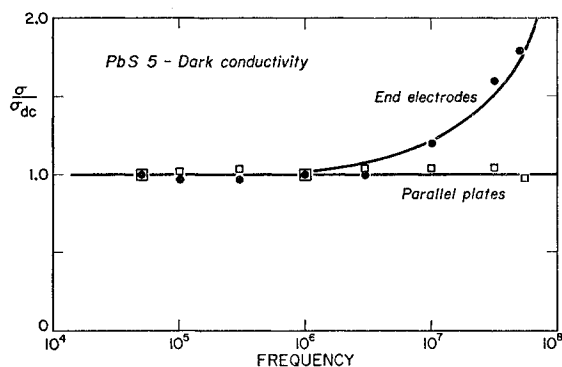


FIG. 2. Comparison of apparent conductivity of PbS film as measured using conventional end electrodes with the conductivity measured in the uniform electric field produced by parallel plates.

⁷ R. P. Chasmar, *Nature* **161**, 281 (1948).

⁸ R. Broudy and H. Levinstein, *Phys. Rev.* **94**, 285 (1954); **94**, 290 (1954).

⁹ E. S. Rittner and F. Grace, *Phys. Rev.* **86**, 955 (1952).

¹⁰ M. Lax and R. Sachs, *Phys. Rev.* **107**, 650 (1957).

¹¹ J. N. Humphrey, F. L. Lummis, and W. W. Scanlon, *Phys. Rev.* **90**, 111 (1953).

apparent increase in conductance which is obtained with end electrodes is eliminated completely with the parallel plates. As is discussed below, one has to go to frequencies about 100 Mc/sec with these films to observe a genuine increase in film conductance.

The measurements described in this paper were performed on twelve samples. Eight of these were experimental films, developed to give as wide a range in film response as possible. Four films were of commercial quality. Surface conductivity of the films varied by almost two orders of magnitude and photoconductivity varied by well over three orders of magnitude. No measurement of the film thickness is available so that direct comparison of the conductivities of the films is not possible, but all films were probably about 0.5 micron thick. In order to minimize high-frequency losses from the substrate material, most of the NOL samples were deposited on Vycor. The E-K samples were deposited on quartz blanks. Since the general behavior of the samples on Vycor and quartz was entirely similar to those on soda glass, the usual substrate material, it is doubted that the substitution of these substrates introduced any systematic effects.

The measurement of dark conductivity vs frequency required the use of four different kinds of techniques. Measurements on each sample were always made in the same order: uhf measurements at 300 Mc/sec and 900 Mc/sec, rf measurements (50 kc/sec to 50 Mc/sec); dc measurements, and finally microwave (9 kMc/sec) measurements. This order was dictated by the size of samples needed in each measurement, since for each measurement the sample was cut down from that used in the previous one. The same film was used in order to minimize as much as possible effects due to variation in sample composition. Typically the samples varied in size from about 1.5×2.5 cm for the uhf measurements to about 0.25×0.25 cm for the microwave measurements. At worst the dc dark conductivity of one film varied over the surface by about 25%.

A. dc Measurements

The dc measurements consisted of determination of dark and photoconductivities and dark and photo-mobilities. Contact to the sample was made with either evaporated gold electrodes to which leads were soldered or by colloidal graphite dissolved in alcohol, which was painted on the sample and to which leads were attached with silver print. Both types of electrodes were Ohmic and noise-free, but because of the ease of application the second technique was more frequently used. The usual dc sample was provided with two current electrodes and two Hall electrodes and was scratched in such a manner that the Hall electrodes were well out on arms of lead sulfide so that there was no noise from current flowing through these electrodes as has been observed by other workers. Figure 1(a) shows a typical sample. Samples were between 0.5 and 1.0 cm in length. Sample lengths

TABLE I. Summary of results of measurements.

Sample	σ_{dc} (sq/Ω)	$(\Delta\sigma/\sigma)_{dc}^a$	$\sigma_{\mu w}/\sigma_{dc}$	f_1 (cps)	$(\Delta\sigma_1/\Delta\sigma_{dc})$	$(\Delta\sigma_{\mu w}/\Delta\sigma_{dc})$	μ_{dc} (cm ² /v-sec)	$\mu_{\mu w}^{dark}$ (cm ² /v-sec)	$\mu_{\mu w}^{photo}$ (cm ² /v-sec)	τ (μ sec)
PbS 1	6.0×10^{-7}	...	17	4.3	1.3
PbS 5	5.5×10^{-6}	...	4.0	1.2×10^9	0.49	2.0	52	5
PbS 14	3.3×10^{-6}	8.2×10^{-2}	7.0	1.6×10^8	2.8	1.8	9.4	19	27	20
PbS 16	7.2×10^{-6}	1.2×10^{-1b}	6.5	1.6×10^8	1.2	0.42	16	5.1	-17	5
PbS 17	5.2×10^{-5}	1.2×10^{-2b}	6.5	1.3×10^8	1.2	0.68	11	8.7	200	≤ 2
PbS 19	3.4×10^{-6}	3.1×10^{-2}	4.0	3.0×10^8	3.5	0.63	11	1.9	-65	5
PbS 20	4.9×10^{-6}	3.2×10^{-2b}	2.8	0.81	4.5	3.0	55	≤ 2
PbS 21	3.6×10^{-6}	8.9×10^{-3b}	3.2	1.1	4.2	3.8	240	≤ 2
PbS 23	1.8×10^{-6}	2.4	8.2	1.0×10^8	1.8	1.0	8.9	8.3	11	450
PbS 24	3.6×10^{-6}	2.5	3.5	1.5×10^8	2.0	0.96	9.2	16	21	410
PbS 25	3.4×10^{-6}	2.6	3.4	0.53	8.0	7.8	24	370
PbS 26	1.5×10^{-6}	3.9	3.3	3.5×10^8	3.0	1.4	6.7	17	19	560

^a $\Delta\sigma/\sigma$ measured with sample mounted in microwave cavity for dc measurements, 2v on lamp except those marked (b).

^b Lower sensitivity samples illuminated with 6v on lamp.

and widths were measured with a stereo microscope equipped with an eyepiece comparator. The voltage applied across the sample was usually 3 v.

B. rf Measurements

Measurements of conductivity and photoconductivity in the range from 50 kc/sec to 50 Mc/sec were made using a Boonton Q meter, Type 260-A. As was mentioned above, previous measurements in this frequency range showed a conductivity which increased with frequency due to self-capacitance effects. In order to avoid this difficulty, a parallel plate capacitor was constructed and mounted on the Q meter. The sample to be measured was placed between the plates extending from one to the other and electrically attached to the plates. In order that losses from the capacitor itself would be negligible, it was constructed of polished copper plates separated by Teflon spacers. Using this geometry self-capacitance effects were eliminated. In order to check that the sample backing was not contributing to the losses, runs were made using the various backing materials with the PbS scraped off. Loss due to the backing was found to be completely negligible in the radio-frequency range.

C. uhf Measurements

Measurements of conductivity and photoconductivity were made at 300 and 900 Mc/sec by Q measurements in a coaxial cavity operated at $\lambda/2$ and $3\lambda/2$ and at 900 Mc/sec in a rectangular cavity operated in a TE_{101} mode. The coaxial cavity had two slots in its outer wall, one for inserting the sample and the second for illumination of the sample. In position, the sample extended from the center post to the outer wall of the cavity. The empty coaxial cavity had an unloaded Q of 600 at 300 Mc/sec and 1300 at 900 Mc/sec. The rectangular cavity was approximately 10 inches square and $\frac{1}{2}$ inch high. A slot was provided in the center of one of the square surfaces for insertion of the sample. In position the sample extended from one square wall to the other. A slot for illumination was provided opposite the sample

in an end wall of the cavity. The empty-cavity unloaded Q was approximately 3800. The cavities were loop coupled and operated in transmission. Power was obtained from a General Radio Type 1021-P2-uhf signal generator.

Measurements of the cavity Q were made with the sample in the cavity and with it replaced by an identical piece of the substrate material. From the change in Q between these two measurements the sample conductivity was calculated using an appropriate filling factor. Unfortunately, it was impossible to calculate a reliable filling factor for the geometry used in the coaxial cavity. This is mainly because the sample destroys the cylindrical symmetry of the field in the cavity. However, the filling factor for the rectangular cavity was easily calculated because of the simple geometry used. Comparison between measurements at 900 Mc/sec made in the two cavities yielded a filling factor for the coaxial cavity which was then used at 300 Mc/sec. It should be noted that in neither cavity need depolarizing effects be considered since the sample was in contact at its ends with the cavity walls.

D. Microwave Measurements

Microwave measurements of dark and photoconductivity were also made by determining Q values. Measurements of dark and photo-Hall mobilities were made by the technique of microwave Faraday rotation. The cavity used was a cylindrical bi-modal transmission cavity operated in a TE_{111} mode. X-band microwave power was obtained from a reflex klystron which delivered approximately 50 mw of power. In order to measure sample conductivity, the cavity Q was measured both with the sample mounted on styrofoam at the center of the cavity and with an equivalent piece of the backing material replacing the sample. The reduction of the field at the sample and hence the reduction of sample loss due to depolarization effects in the sample backing were accounted for theoretically.

The variation of the dark conductivity with frequency was qualitatively similar for all films studied. The con-

ductivity was constant at low frequencies, increased in the region of 100 Mc/sec and was then again constant out to 10 kMc/sec. The quantity f_3 listed in Table I is that frequency at which the conductivity had risen to $(\sigma_{\mu w} + \sigma_{dc})/2$ and hence is an indication of the frequency at which the rise in conductivity occurs. The ratio of the conductivity at microwave frequency to that at dc, $\sigma_{\mu w}/\sigma_{dc}$, varied from 2.8 to 17. For most samples the value of this ratio fell between 3 and 8. In the lower half of Figs. 3, 4, and 5 is shown the variation in dark conductivity with frequency. The films PbS 14 and PbS 19 are experimental NOL films. PbS 14 is a moderately sensitive film; PbS 19 is somewhat less sensitive. PbS 23 was provided by Eastman-Kodak and is an exceptionally sensitive film. The circles show the experimental data and the solid curve drawn through them is a theoretical curve based on the model to be described in Sec. VI. The scatter of the experimental points in these figures is fairly typical.

Of course, the striking feature of the dark conductivity measurements is the abrupt rise in conductivity over a

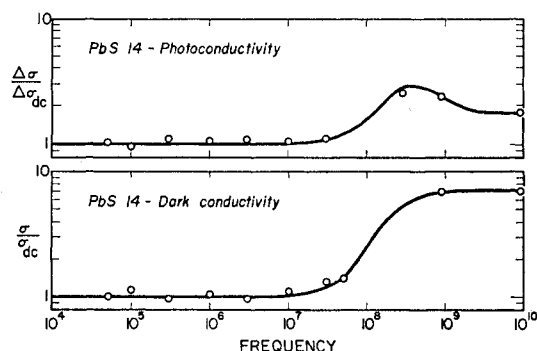


FIG. 3. Variation of conductivity and photoconductivity with frequency for PbS 14, the most sensitive NOL film.

decade in the vicinity of 100 Mc/sec. This sharp rise in conductivity is typical of material with well-resolved regions of differing conductivity. These measurements give clear and striking support to the idea that thin high resistivity barriers are present in these films. If one were to represent the barriers by a resistance and capacitance in parallel, then the frequency f_3 is roughly equal to $\frac{1}{2}\pi\epsilon\rho$ where ρ is the barrier resistivity and ϵ is the dielectric constant. Even with a dielectric constant of ten this result implies a barrier resistivity as high as 5×10^8 ohm-cm. The resistivity of intrinsic PbS at room temperature is probably no more than one hundred ohm-cm so that at first sight the calculated barrier resistance appears remarkably high. It was this kind of result that led Petritz to suggest that the barriers may be a high-resistivity oxide rather than $p-n$ junctions. Actually, this kind of estimate can be misleading. As we shall see later, for the model we describe, the frequency f_3 is not related to the barrier resistivity at all but depends on intrinsic film properties. The surface conductivity meas-

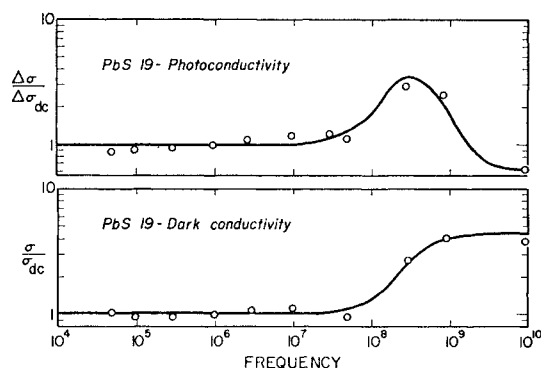


FIG. 4. Variation of conductivity and photoconductivity with frequency for PbS 19, a relatively insensitive NOL film.

ured at microwave frequencies implies a range of bulk resistivity between 1 and 10 ohm-cm for the twelve films studied. There does not seem to be any particular correlation between this quantity and film sensitivity.

III. PHOTOCONDUCTIVITY

Photomeasurements were usually made by chopping the light at 16 cps although the most sensitive samples were examined with a dc system. When chopped light was used the signal from the sample was amplified with a calibrated narrow band ac amplifier and synchronously detected with a diode lock-in. Measurements of photoconductivity in the uhf range were made in the two cavities described in Sec. IIC by setting the signal generator at the cavity resonant frequency and measuring the change in transmitted power with the sample illuminated. In the measurements at microwave frequencies the sample was illuminated through a small hole in the back of the input waveguide opposite the coupling iris. Measurements in the rf range were made with unchopped light by noting the change in Q on the Q meter. In all instances, except for the pulsed light measurements to be described later, an 18-amp 6-volt tungsten ribbon filament lamp was used as a light source and operated at 2, 4, or 6 volts depending on the sample photoconductivity. The responsivity $\Delta\sigma/\sigma$ was usually

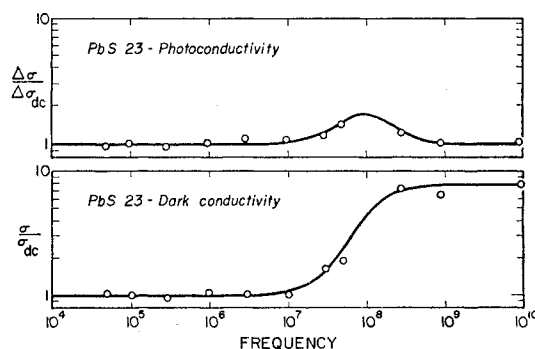


FIG. 5. Variation of conductivity and photoconductivity with frequency for PbS 23, a sensitive Eastman-Kodak film.

kept below 10 or 15%. The increase in conductivity is given in the second column of Table I. During the early measurements a quartz prism monochromator was used to investigate the responsivity of several samples as a function of the wavelength of the incident radiation. In no case did this spectrum differ with the frequency of the ac voltage on the film. In addition to the ac photoconductivity described above, the dc photoconductivity was measured after each run with the sample in the same position as for the higher frequency photoconductivity. In this way variation of light intensity between the various setups could be accounted for.

The variation of photoconductivity with frequency was qualitatively similar for all samples measured. It was constant at low frequencies, rose to about twice the dc value at a frequency equal to f_3 and then dropped at 10 kMc/sec to a value comparable to the dc value. More specifically the photoconductivity at microwave frequency varied from 0.42 to 1.8 times that at dc. The column headed $\Delta\sigma_{\mu w}/\Delta\sigma_{dc}$ in Table I gives this quantity for all samples measured. In addition, the value of the photoconductivity at f_3 normalized to the dc value is given in the column headed $\Delta\sigma_3/\Delta\sigma_{dc}$. In the upper half of Figs. 3, 4, and 5 is shown the variation of photoconductivity with frequency for films PbS 14, PbS 19, and PbS 23, respectively.

If one were to regard the films as composed of material of resistivity of a few ohm-cm separated by barriers of resistivity of 10^4 ohm-cm, one could account for the frequency dependence of the dark conductivity. With photoexcitation in the low resistivity regions one should expect a sample response just equal to the fractional increase in carrier concentration. That is, the curves of conductivity and photoconductivity should be similar. Such is clearly not the case. On the other hand, if the effect of the light were to modify the barrier resistivity, then the photoconductivity should drop to zero at high frequencies where the barriers are shorted out by their shunt capacitance. Instead the experiments indicate that the photoconductivity is relatively constant at high frequencies at a level comparable to the dc level. One could begin to speculate at this point about film structures which might lead to results of the kind observed here. We will postpone this though until we have discussed the mobility measurements, which are equally puzzling on either of the standard models.

IV. dc HALL MOBILITY

The dc Hall mobility measurements were made with the sample mounted in the gap of a small electromagnet capable of producing magnetic fields up to 6000 oersteds. All mobility measurements were made at maximum field strength. The magnet was provided with a hole through one of its poles and a lens system was set in this hole for focusing the image of a tungsten lamp onto the sample. Measurements of dark and photoconductivity and mobility were made with sample mounted in this way.

The sample current and Hall voltage was measured using a Hewlett-Packard Model 425A dc micro-voltammeter whose output was recorded on a strip chart. Photomeasurements were usually made by chopping the light at 16 cps, although when the photoconductivity was large it was sometimes measured with the dc system. When chopped light was used, the signal from the sample was amplified with a calibrated narrow band ac amplifier and synchronously rectified with a diode lock-in as for the conductivity measurements.

The value of the Hall mobility at dc varied from 0.49 to 15.8 cm²/v-sec and all samples were *p* type. These values are consistent with previously published results on chemically deposited films. The Hall mobility of the E-K films varied considerably less than this ranging from 6.7 to 9.2 cm²/v-sec. No particular attempt was made with all samples to check Woods' result⁶ that the change in the Hall mobility on illumination of the sample was considerably smaller than the change in conductivity. However, in several samples, which showed a small photoconductive signal across the Hall electrodes, it was possible to make this check. For PbS 14, $\Delta\mu/\mu \leq 1.4 \times 10^{-3} \Delta\sigma/\sigma$; for PbS 17, $\Delta\mu/\mu \leq 1.2 \times 10^{-1} \Delta\sigma/\sigma$; and for PbS 24, $\Delta\mu/\mu \leq 4.7 \times 10^{-2} \Delta\sigma/\sigma$, which results confirm Woods' findings. Due to the general similarity of all films, we can be fairly certain that this was also true for the other samples even though the photoconductive signal across the Hall electrodes was too large to be able to measure easily an additional small signal when the magnetic field was turned on.

Woods has analyzed his data on a model which assumes that the current is limited by barriers. If we take the barriers to be of height $e\phi_0$ and assume that the voltage V across each barrier is small compared with kT one can easily show that the barrier conductance per unit area is given by

$$j/V = p \exp[-e\phi_0/kT] e^2/\pi m \langle v \rangle, \quad (1)$$

where $\langle v \rangle$ is the mean carrier velocity within the bulk material, p is the hole concentration, and m is the carrier mass. Under these circumstances the sample conductivity is simply

$$\sigma = jd/V,$$

where d is the mean distance between barriers. If one now applies a magnetic field perpendicular to the film, a Lorentz force will act on the drift current. If the barriers are thin compared with their mean separation d , we can neglect the Hall current within the barrier and concentrate on the force acting on the carriers within the crystallites. Without any opposing electric fields there will be a transverse force per carrier

$$F = jH/pc.$$

There will be a development of surface charge setting up an opposing electrostatic potential across the crystallite:

$$eV_H = Fd.$$

It should be noted that whereas the potential drop which produces the drift current appears across the barriers, the potential drop which opposes the Hall current appears across the interior of the crystallites. The Hall angle, which is the ratio of these two voltages, is given by

$$\Theta_H = V_H/V = (1/\pi)(eH/mc)(d/\langle v \rangle) \times \exp[-e\phi_0/kT]. \quad (2)$$

One can define an apparent Hall mobility from the expression

$$\theta_H = \mu_H H/c,$$

which is just the same expression that we obtain from the apparent drift mobility given from

$$\sigma = p e \mu_D.$$

For this reason it is not necessary to make any distinction between the apparent Hall and drift mobilities in these structures. If one now considers the effect of illumination, one can write that the fractional increase in sample conductivity is given by

$$\Delta\sigma/\sigma = \Delta p/p \Delta\mu/\mu.$$

Our experiments are in agreement with those of Woods in placing the second term below 10% of the first term. Actually this is an upper limit and the second term may be as small as 10^{-3} of the first term. While we agree with Woods that the carrier mobility is not photo-dependent, we cannot accept his model for reasons which have been stated earlier. A more general conclusion from his result would be that the distribution of electric fields and currents within the film is not affected by light. Under these circumstances all currents which were flowing in the dark are increased by the same fraction. The change in current is then exactly the same as if the electric field were increased in magnitude. Therefore, the Hall angle must remain unchanged with illumination. We shall see in Sec. VI how the model which we wish to propose gives this result automatically.

V. MICROWAVE HALL MOBILITY

For the photoconductivity and mobility measurements at microwave frequencies the microwave cavity was placed between the poles of the electromagnet used for the dc measurements and described earlier. The same optical arrangement as for the dc measurements was used with the sample illuminated through a small hole in the back of the input waveguide opposite the coupling iris.³ With this arrangement the magnetic field was along the axis of the cavity and was coaxial with the direction of the incident light.

The Hall mobility for dark carriers at microwave frequency was also p type for all samples but varied over a larger range than did the dc Hall mobility, the largest value being $19 \text{ cm}^2/\text{v-sec}$. There seems to be no particu-

lar correlation between the relative values of the Hall mobility at dc and 10 kMc/sec and other film properties.

The Hall mobility for photocarriers at 10 kMc/sec showed more variation than the other quantities and showed a correlation with the photosensitivity of the film, being large in absolute value in insensitive films. It was p type for all samples except two of those from NOL. The largest values of this quantity were found for two insensitive NOL films, PbS 17 and PbS 21. The films with the n -type photomobilities were PbS 16 and PbS 19. The more photosensitive films generally had a photomobility of the same order as the dark mobility. For all films the magnitude of the microwave photomobility was somewhat greater than either the dc or microwave dark mobilities. It is clear that any barrier limited model would have to give an increase in Hall mobility at microwave frequencies just equal to the increase in conductivity. At microwave frequencies the barriers are shorted out by their shunt capacitance and all the potential drop appears across the interior of the crystallites. Similarly, the microwave Hall current is unimpeded by barriers. We should then measure essentially a bulk mobility. Since the dark mobilities which we measure at microwave frequencies do not increase by anything like the increase in conductivity, we must conclude that barriers have relatively little to do with the determination of the dc Hall mobility. This means that the dc current must flow through channels in which the bulk mobilities are of the order of magnitude of the observed mobilities, about $10 \text{ cm}^2/\text{volt-sec}$. One apparent difficulty in the suggestion that the hole mobilities in PbS may be as low as $10 \text{ cm}^2/\text{volt-sec}$ is that this runs counter to the general assumption that the mobilities in films are of the order of the bulk lattice mobility, $600 \text{ cm}^2/\text{volt-sec}$. We see no other conclusion, however, especially in view of the fact that the bulk conductivity of the films, measured at microwave frequencies, falls short of even the intrinsic conductivity. It does not seem unreasonable physically that the films may contain sufficient impurities to limit the mobility to values of the order observed. Early values of the Hall mobility in both natural and synthetic PbS crystals have been given by Eisenmann¹² who observed Hall mobilities covering a wide range with some samples showing Hall mobilities as small as $10 \text{ cm}^2/\text{volt-sec}$. These values were presumably majority carrier mobilities since the carrier concentrations observed for these samples were much greater than the intrinsic value.

VI. PROPOSED FILM STRUCTURE

The observed frequency dependence of the dark conductivity and the photoconductivity and the comparison between dc and microwave Hall mobilities, run counter to what one would expect from a barrier model of PbS films. Although the dark conductivity appears to give evidence for barriers, the photoconductivity does

¹² L. Eisenmann, Ann. Physik. 430, 121 (1940).

not. Similarly, if the dc Hall mobility were barrier limited, one would expect much higher microwave Hall mobilities than are observed. It appears to us that the only way in which one can have a photoconductivity which is relatively independent of frequency while the dark mobility increases strongly with frequency is to have the photoconducting channels in shunt with the isolated insensitive regions. It would appear superficially that a model in which all the photocurrent is taken to flow at the film-glass or film-air interface would satisfy this requirement. One would consider that this surface material is barrier free and that the current flows over the surface while the rest of the film is interrupted by barriers. This model would give the observed frequency variation of the dark conductivity. It would give a photoconductivity relatively independent of frequency although the hump in the photoconductivity would remain unexplained. It would also give equal dark and photomobility at dc since only surface current would be observed. One could still account for the low microwave dark mobility only by assuming low bulk mobilities as we have argued. Perhaps the main drawback of this model, apart from the fact that the hump in the photoconductivity is unexplained, is that it gives a microwave photomobility which is identically equal to the dc mobility. Wide discrepancies from this rule are found among the NOL films with some of the microwave photomobilities over an order of magnitude higher than the dc mobilities. Even for the high sensitivity E-K films the photomobilities are as much as three times higher than the dc mobility.

We were led to an alternative model of PbS films in an effort to explain the hump in photoconductivity. We argued that the hump comes in the frequency region where the film conductivity is increasing and so is especially sensitive to the barrier shunt capacitance. This suggests that the hump in photoconductivity is a modulation of the barrier capacitance. The barrier modulation model gives this result automatically. However, we have argued that the dc mobility cannot be barrier limited. A model which seems to satisfy all the restrictions which we have placed on it is shown in Fig. 6. The conducting channels are shown in white. They extend through the material continuously. The interiors of the isolated regions are shown dotted and the solid lines are barriers. We assume that only the channels are photosensitive and the interior is insensitive. The channels shunt the crystallites as the photoconductivity measurements suggest. But they are also in series with the crystallites. Then the barriers are always between isolated insensitive and nonisolated photosensitive material.

Associated with the barrier between the insensitive and photosensitive regions will be a space charge region which we require to be a depletion layer in the photosensitive region. The extent of this depletion region will be of the order of the Debye length $L_D = (\epsilon kT / 4\pi p_2 e^2)^{1/2}$. Here p_2 is the carrier concentration in the photosensitive

region. For $p_2 = 10^{17}/\text{cm}^3$, $L_D = 1.6 \times 10^{-6}$ cm, approximately $\frac{1}{6}$ of the average crystallite size. Thus carriers in the photosensitive region are forced to remain a distance L_D from the actual barrier.

When photocarriers are excited, p_2 will increase and consequently L_D will decrease. Thus the carriers in the photosensitive area may come closer to the barrier. Consequently, the capacitance across the barrier increases. On this simple picture we obtain

$$\Delta C/C = -\Delta L_D/L_D = \Delta p_2/2p_2 \quad (3)$$

provided the length determining the capacitance is the dimension of the space charge region itself.

The effect of this capacitance modulation will be seen in the variation of the photoconductivity vs frequency. At low frequency a negligible amount of current will flow across the barrier and a modulation of the capacitance will have no effect. At very high frequencies the reactance of the barrier is much smaller than the resistance of the regions in series with it, and hence it does not limit the current. Consequently, a capacitance modulation will have no effect at these frequencies either. However, at intermediate frequencies where the reactance of the barrier is comparable to the resistance of the other regions in series with it, we expect an increase in the capacitance to cause an increase in the current. Thus the broad rise at intermediate frequencies seen in the photoconductivity may arise from a modulation of the width of the barrier.

As we shall see, this geometry permits a difference between the microwave photomobility and the dc mobility as is required by experiment. This is because at least some of the photo-Hall current must flow through the insensitive regions. By regarding the mobility within the isolated regions as adjustable, we fit all the data with the exception of the microwave photomobility. We then calculate the microwave photomobility from our model and compare the calculated values with those obtained from experiment. As we shall see in Sec. VII the agreement between the calculated values and those observed for the sensitive films is quite good. On the other hand, there are reasonably large discrepancies in the case of the insensitive films. This may be because of the neglect of the photoconductivity of the isolated regions. However, since the model which we propose does satisfac-

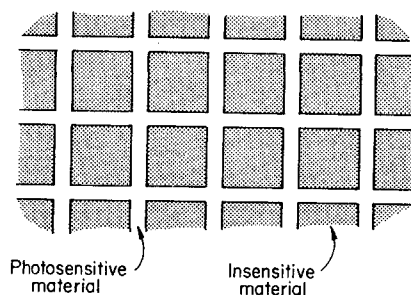


FIG. 6. Two-dimensional diagram of model used for calculation.

torily account for the main features of all the films examined we will proceed with a detailed calculation neglecting any photoexcitation within the isolated regions.

The basic unit we shall consider for this calculation is that shown in Fig. 7 and consists of a cube with side l_1 surrounded by a barrier and filled with material of conductivity $\sigma_1 = p_1 e \mu_1$ surrounded on three sides by a layer of thickness l_2 of material with conductivity $\sigma_2 = p_2 e \mu_2$. (The material could be distributed equally on all six sides of the cube but the above configuration is equivalent and more convenient for purposes of calculation.) The barrier separating regions 1 and 2 is indicated by the heavy black line in Fig. 7. At all frequencies we shall assume the current density in the shunt part of region 2 (region 2-*i*) to be uniform throughout the region. This overestimates the conductance of region 2-*i* at dc but since we assume $l_1 \approx l_2$, considerable spreading of the current will occur in this region so that this approximation is reasonable. Thus we may define the following conductances

$$g_1 = \sigma_1 l_1; \quad g_2 = \sigma_2 (l_1 + l_2)^2 / l_2; \quad g_3 = \sigma_2 l_2 (2l_1 + l_2) / l_1, \quad (4)$$

and use the equivalence circuit of Fig. 8. Here C is the capacitance of the barrier separating the two regions and we neglect the conductance of the barrier.

The calculation of the conductance of this circuit follows in a straightforward manner. We obtain

$$G = \frac{g_1^2 g_2 g_3 (g_2 + g_3) + \omega^2 C^2 g_2 (g_1 + g_3) (g_1 + g_2 + g_3)}{g_1^2 (g_2 + g_3)^2 + \omega^2 C^2 (g_1 + g_2 + g_3)}. \quad (5)$$

At $\omega = 0$ we find $G_0 = g_2 g_3 / (g_2 + g_3)$ and as $\omega \rightarrow \infty$ $G_\infty = g_2 (g_1 + g_3) / (g_1 + g_2 + g_3)$. It is convenient to define a dimensionless frequency

$$\gamma = \omega C (g_1 + g_2 + g_3) / g_1 (g_2 + g_3), \quad (6)$$

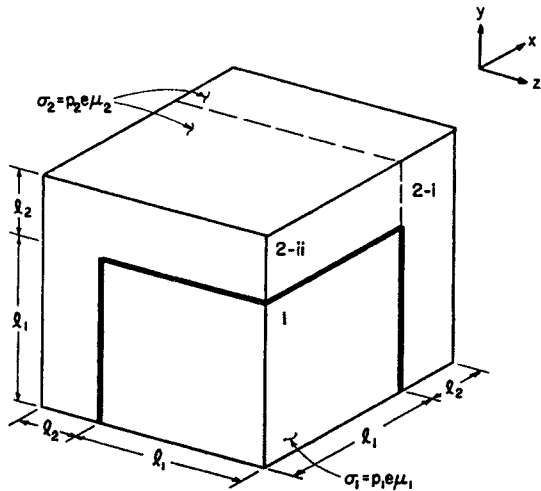
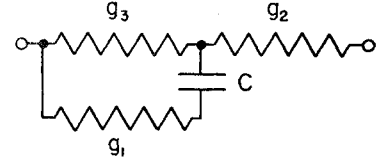


FIG. 7. Basic unit used for calculation. Region 1 is taken to be insensitive. Region 2 is taken to be photosensitive. The heavy black line represents a barrier. Current flow is taken to be in the x direction.

FIG. 8. Equivalent circuit for calculation of conductance of structure shown in Fig. 7.



in terms of which we find

$$G = (G_0 + \gamma^2 G_\infty) / (1 + \gamma^2). \quad (7)$$

Note that at $\gamma = 1$, $G = (1/2)(G_0 + G_\infty)$ the average of low- and high-frequency conductances. We define the corresponding frequency as ω_1 .

As stated above we assume the photoconduction to take place only in region 2, hence only in g_2 and g_3 . For small photoexcitation, the photoconductivity will be given by

$$\Delta G = (\partial G / \partial g_2) \Delta g_2 + (\partial G / \partial g_3) \Delta g_3 + [\partial G / \partial (\omega_1 C)] \Delta (\omega_1 C). \quad (8)$$

If we assume $g_3 \ll g_1, g_2$ and write these derivatives in terms of γ as defined above, we find

$$\partial G / \partial g_2 = [(g_3 / g_2)^2 - \gamma^2 g_1^2 / (g_1 + g_2)^2 + \gamma^4 g_1^2 / (g_1 + g_2)^2] / (1 + \gamma^2)^2, \quad (9)$$

$$\partial G / \partial g_3 = \{1 + [\gamma^2 / (g_1 + g_2)^2] [2g_2 (g_1 + g_2) - g_1^2] + \gamma^4 g_2^2 / (g_1 + g_2)^2\} / (1 + \gamma^2)^2, \quad (10)$$

$$\partial G / \partial (\omega_1 C) = 2\gamma^2 / (1 + \gamma^2)^2. \quad (11)$$

Here $\omega_1 C$ is given by

$$\omega_1 C = g_1 g_2 / (g_1 + g_2). \quad (12)$$

We note that since g_2 and g_3 both consist of material of conductivity σ_2 it is necessary that $\Delta g_2 / g_2 = \Delta g_3 / g_3$. For simplicity we may take a unit increase in conductance: $\Delta g_2 = g_2$ and $\Delta g_3 = g_3$. Then

$$\Delta G_0 = g_3, \quad \Delta G_\infty = g_1^2 g_2 / (g_1 + g_2)^2, \quad (13)$$

provided $g_3 \ll g_1, g_2$. Also, with this approximation

$$G_0 = g_3, \quad G_\infty = g_1 g_2 / (g_1 + g_2). \quad (14)$$

For the calculation of the mobility we may use an equivalent circuit approach similar to that used in calculating the conductance. For any homogeneous region a transverse Hall field E_T is set up given by

$$E_T = (\mu H / c) E_L, \quad (15)$$

where E_L is the longitudinal (in the direction of current flow) field in that region. Written in terms of the longitudinal voltage V_L applied across the region, the transverse open circuit voltage V_T will be

$$V_T = (\mu H / c) V_L l_T / l_L, \quad (16)$$

where l_T and l_L are the dimensions of the region in the transverse and longitudinal directions. If, in addition, a transverse current i_T flows in the region, the voltage

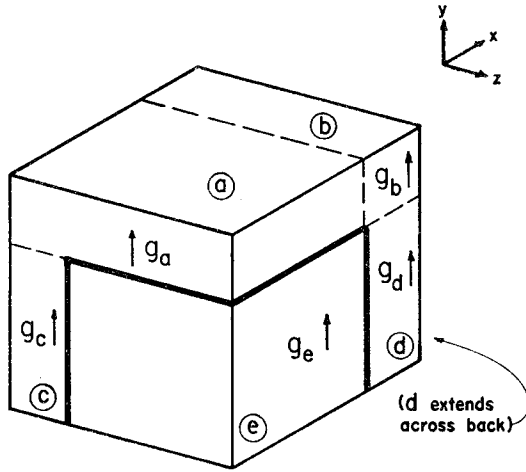


FIG. 9. Subdivision of basic unit for Hall mobility calculation. Current is taken to flow in the x direction and the magnetic field is taken in the z direction.

drop due to this flow will be i_T/g_T , where g_T is the transverse conductance of the region. Hence, the equivalent circuit for the region for the determination of the Hall voltage is simply g_T in series with V_T . One of these voltage and conductance combinations will hold for each homogeneous region of our inhomogeneous model and they may be combined in series and parallel as required.

We divide the basic unit used for the conductance calculation into five subdivisions with the transverse conductances g_a through g_e as shown in Fig. 9. Clearly we may write these transverse conductances in terms of the longitudinal conductance as follows:

$$\begin{aligned} g_a &= g_2 l_1 / (l_1 + l_2), & g_b &= g_2 l_2 / (l_1 + l_2), \\ g_c &= g_3 l_1 / (2l_1 + l_2), & g_d &= g_3 (l_1 + l_2) / (2l_1 + l_2), & g_e &= g_1. \end{aligned} \quad (17)$$

To be consistent with the circuit for longitudinal current, the equivalent circuit for transverse current will consist of g_c and g_d in parallel and in parallel with the series combination of g_e and C . This combination will be in series with the parallel combination of g_a and g_b . This circuit is shown including the appropriate transverse voltages in Fig. 10.

We have mobility data only at dc and at microwave frequencies so we shall be interested only in the calculation of the Hall mobility in the high- and low-frequency limits. The high-frequency Hall mobility may be calculated using the circuit of Fig. 10 with C short circuited. The low-frequency calculation will follow directly from this result by setting $g_1 = 0$, i.e., by allowing no current flow in the region 1. With C short circuited the longitudinal voltages across the various regions i (i takes on the values a through e) are determined from the current equivalent circuit and the transverse voltage are obtained from them by using $V_{T,i} = (\mu H / C) V_{L,i} \times l_T / l_L$ in each region. Using these, the transverse voltage V_T across the terminals of the Hall equivalent circuit is

calculated and finally the Hall mobility μ_H is obtained from $\mu_H = (c/H) V_T / V_L$. We find

$$\begin{aligned} \mu_H^{\mu\omega} &= \mu_2 \left\{ \frac{\lambda}{1+\lambda} + \frac{g_3}{g_1 + g_2 + g_3} \frac{1+\lambda}{\lambda(2+\lambda)} \right. \\ &\quad \left. + \frac{g_1 g_3}{(g_1 + g_3)(g_1 + g_2 + g_3)} \frac{1}{2+\lambda} \right\} \\ &\quad + \mu_1 \frac{g_1 g_2}{(g_1 + g_3)(g_1 + g_2 + g_3)}. \end{aligned} \quad (18)$$

Here $\lambda = l_2 / l_1$. Setting $g_1 = 0$ we obtain for the dc Hall mobility

$$\mu_H^{dc} = \mu_2 \left\{ \frac{\lambda}{1+\lambda} + \frac{g_3}{g_2 + g_3} \frac{1+\lambda}{\lambda(2+\lambda)} + \frac{g_2}{g_2 + g_3} \frac{1}{2+\lambda} \right\}. \quad (19)$$

The mobility $\mu_{\mu\omega}^{\text{photo}}$ of photoexcited carriers at microwave frequency is defined as

$$\mu_{\mu\omega}^{\text{photo}} = (c/H) \Delta \sigma_{xy} / \Delta \sigma_{xx}, \quad (20)$$

or consequently under constant field conditions

$$\mu_{\mu\omega}^{\text{photo}} = (c/H) \Delta j_T / \Delta j_L, \quad (21)$$

where Δj_T is the change of the transverse short circuit current density on illumination and Δj_L the change of the longitudinal current density. Making this calculation we obtain

$$\begin{aligned} \mu_{\mu\omega}^{\text{photo}} &= \mu_2 \left\{ \frac{\lambda}{1+\lambda} + [g_3^2 (3g_1 + g_2 + g_3) + 2g_1 g_2 g_3] \frac{1+\lambda}{\lambda(2+\lambda)} \right. \\ &\quad \left. + g_2 g_3 (3g_1 + g_2 + g_3) \frac{1}{2+\lambda} + \frac{\mu_1}{\mu_2} 2g_1^2 g_2 / \right. \\ &\quad \left. \times [g_3 (g_1 + g_2 + g_3) + g_1 (g_1 + g_3)] \right. \\ &\quad \left. \times (g_1 + g_2 + g_3) \right\}. \end{aligned} \quad (22)$$

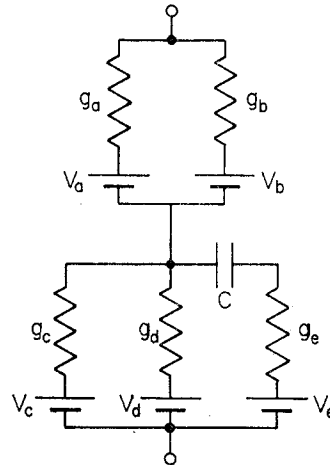


FIG. 10. Equivalent circuit for calculation of Hall mobility.

VII. COMPARISON WITH EXPERIMENT

In comparing our experimental results with the calculation above we shall treat two distinct groups of samples. First are the photosensitive samples PbS 23, 24, 25, 26, the E-K samples, and PbS 14, the one NOL film prepared to yield optimum photosensitivity, and second are the other NOL films all of which were deliberately prepared off optimum. We shall see that the data on the first group agree well with the results obtained above. The second group does not fit well and we shall discuss probable reasons for this.

In calculating the values of g_1 , g_2 , and g_3 needed to fit the experimental results we use the approximate expressions for G and ΔG from Eq. (13) and Eq. (14) for convenience. In all cases the values so derived when substituted into the exact expression for G and ΔG yield the correct results to within 10%. We shall be satisfied with results to this accuracy. Hence, using these approximate expressions

$$\frac{g_3}{G_0} = 1; \quad \frac{g_2}{G_0} = \left(\frac{G_\infty}{G_0} \right)^2 \frac{\Delta G_0}{\Delta G_\infty}; \quad \frac{G_0}{g_1} = \frac{G_0}{G_\infty} - \frac{G_0}{g_2}. \quad (23)$$

In Table II we show the values of g_1 and g_2 obtained by this procedure. Also shown is the ratio of the dimensions of the two regions, $\lambda = l_2/l_1$. This quantity is obtained from the ratio

$$g_2/g_3 = (1+\lambda)^2/\lambda^2(2+\lambda). \quad (24)$$

The other additional quantity needed to fit the data for the photoconductivity as a function of frequency is $\Delta(\omega_3 C)/\Delta G_0$. This quantity is determined by fitting the value of the photoconductivity at $\omega = \omega_3$. Hence, the value of $\Delta(\omega_3 C)/\omega_3 C$ may be calculated. These values are also shown in Table II. Except for PbS 23, these values are somewhat larger than we would expect since, as we have seen from Eq. (3), $\Delta C/C = \Delta p_2/2p_2 = \Delta g_2/2g_2 = \frac{1}{2}$. However, since this expression was derived assuming a plane parallel configuration for the plates of the capacitor, values of $\Delta C/C$ somewhat larger than one half are not unreasonable. For instance, if the interface between the barrier and the photosensitive region were rough on a scale comparable to the Debye length in the dark material, the effective area of the capacitance would increase on illumination as the Debye length became less than the scale of the roughness. Hence, the increase in capacitance would be greater than that predicted from a calculation based on a plane

TABLE II. Values of parameters of model as calculated for sensitive samples.

Sample	g_1/G_0	g_2/G_0	λ	$\Delta C/C$
PbS 14	9.4	27	0.14	0.77
PbS 23	9.4	67	0.093	0.37
PbS 24	4.8	12.8	0.23	0.90
PbS 25	4.1	21	0.17	...
PbS 26	4.5	7.9	0.31	0.84

parallel geometry. The theoretical curves for σ/σ_{dc} and $\Delta\sigma/\Delta\sigma_{dc}$ plotted in Figs. 3 and 5 were obtained using the appropriate parameters shown in Table II. These curves were determined by plotting the curves of conductivity and photoconductivity as a function of the dimensionless parameter γ . An appropriate scale factor was then chosen between γ and ω which made both curves fit the data as well as possible. Also shown in these figures are the experimental points. As can be seen the fit between experiment and theory is quite good.

In fitting the mobility we use the calculated values of g_1 , g_2 , g_3 , and λ in the theoretical expressions. From the experimental values of μ_H^{dc} and $\mu_H^{\omega\omega}$ we determine the values of μ_1 and μ_2 . These values are shown in Table III. Using these values $\mu_{\omega\omega}^{photo}$ is calculated. These results are shown in Table IV compared with the experimental values. Again agreement is seen to be good. Improvement can be obtained for several samples by modifying slightly the experimental results within the range of their accuracy. For instance, for PbS 14, if the value of $\mu_H^{\omega\omega}$ is increased by 10% the theoretical and experimental values of $\mu_{\omega\omega}^{photo}$ are brought within a few percent of each other.

Finally from the data, values of σ_1 , σ_2 , p_1 , and p_2 are calculated. Here we assume all samples to be 0.5μ thick. These quantities are also shown in Table III. There exists considerable scatter from sample to sample in these results, but all of the values obtained are quite reasonable.

The variation of the conductivity and photoconductivity as a function of frequency as given by the above model also describes the behavior of these quantities in the insensitive samples. Figure 4 shows curves of σ/σ_{dc} and $\Delta\sigma/\Delta\sigma_{dc}$ calculated for PbS 19 in the same manner as those for the photosensitive films PbS 14 and PbS 23. As can be seen the fit to experiment of $\Delta\sigma/\Delta\sigma_{dc}$ is not quite as good as for the other samples. It should be noted, however, that this fit can be improved at the

TABLE III. Mobility, conductivity, and carrier concentration calculated for sensitive samples.

Sample	μ_1 (cm ² /v-sec)	μ_2 (cm ² /v-sec)	σ_1 (ohm-cm) ⁻¹	σ_2 (ohm-cm) ⁻¹	p_1 (cm ⁻³)	p_2 (cm ⁻³)
PbS 14	21	13	5.4×10^{-1}	2.4×10^{-1}	1.6×10^{17}	1.1×10^{17}
PbS 23	7.0	14	2.9×10^{-1}	1.9×10^{-1}	2.4×10^{17}	0.83×10^{17}
PbS 24	20	12	2.8×10^{-1}	1.7×10^{-1}	0.90×10^{17}	0.90×10^{17}
PbS 25	6.4	11	2.4×10^{-1}	2.2×10^{-1}	2.3×10^{17}	1.2×10^{17}
PbS 26	8.3	27	1.1×10^{-1}	0.57×10^{-1}	0.24×10^{17}	0.43×10^{17}

TABLE IV. Comparison of experimental and theoretical values of μ_{photo} for sensitive samples.

Sample	Experimental (cm ² /v-sec)	Theoretical (cm ² /v-sec)
PbS 14	27	32
PbS 23	11	12
PbS 24	21	25
PbS 25	24	14
PbS 26	19	18

expense of the fit to $\sigma/\sigma_{\text{dc}}$ by shifting the curves to slightly higher frequency.

The large value of the Hall mobility of the photocarriers at microwaves cannot however be understood on this model. Two samples, PbS 16 and PbS 19 show an n -type photomobility, the only n -type mobilities seen in any samples. In addition, values of the microwave Hall mobility considerably smaller than the dc Hall mobility as seen in several of these samples is not predicted by the above model. Still it should be noted that the general objections to a model in which the dc current must surmount barriers also hold for these insensitive samples.

There exist several possible reasons why these samples are not described as well by our model as are the photosensitive samples. One obvious possibility is related to the fact that these films are less photosensitive. Hence the distinction between photosensitive and non-photosensitive regions becomes impossible. For these samples it would be necessary to consider photoconductivity in region 1 of the model presented above. Qualitatively we can see that such an addition would still not be enough to provide agreement between the model and experiment, since photoconductivity in the interior region would add additional high-frequency photoconductivity. Most of the insensitive samples have a high-frequency photoconductivity lower in magnitude than their dc photoconductivity, a feature in disagreement with our model if there were considerable photoconductivity in region 1. It may be that quenching is important in the low sensitivity films as measured at microwave frequencies. We have not examined the microwave photomobility through the optical spectrum. Such a study might clarify this point.

VIII. OTHER STUDIES

In this final section we discuss several additional physical measurements which may support the proposed model. We have supposed that the same photocarriers are responsible for both the dc and microwave photoconductivity even though their apparent mobilities are somewhat different. In order to verify that the same carriers do dominate the current at both frequencies, we have measured the time constant for the decay of the photocurrent both at dc and at microwave frequencies.¹³

¹³ We are grateful to Dr. R. L. Petritz for suggesting this test of our model.

For measurements of the decay of photoconductivity, light pulses were obtained by chopping the light from a 100-watt zirconium arc lamp with a rotating mirror. The rise and decay times of the light pulse itself were approximately 2 μsec . For measurement of the lifetime at dc the signal from a small resistor in series with the sample was amplified, displayed on an oscilloscope and photographed. At microwave frequency the signal used was that from a detection crystal on the output arm of the cavity.

The value of the time constant τ for decay of photoconductivity at dc varied from sample to sample directly as the photosensitivity $\Delta\sigma/\sigma$ for almost all samples in agreement with the work of Mahlman.¹⁴ The time constant varied from less than 2 μsec for the insensitive NOL samples to 560 μsec for most photosensitive E-K sample, PbS 26. A value of $\tau=20$ μsec was obtained for the most photosensitive NOL sample, PbS 14. The decay was essentially exponential for all samples for low light intensity. In addition, photoconductivity in all samples rose with the light pulse and hence the time constant for photoconductive rise was less than 2 μsec . The close correlation between the measured time constant τ and the photosensitivity $\Delta\sigma/\sigma$ for the various samples shows that increased photosensitivity is simply due to an increased carrier lifetime and lends support to Petritz' suggestion⁴ that minority carrier trapping is responsible for increased sensitivity. To within the error of the measurements, which was small, the time constant was the same at both dc and microwave frequencies, supporting the present model.

Possibly the most direct support for the model proposed here comes from the work of Dutton on fine-spot of PbS films.¹⁵ Dutton has scanned E-K chemically deposited PbS films with an optical resolution of about two microns. He finds a fine structure on the photoconductive signal limited only by his beam resolution. He could well be observing variations as the light beam crosses the photosensitive channels which we have postulated. Evidently polarization effects play a role in Dutton's results so that it would be desirable to measure the microwave photocurrent rather than the dc current.

In summary, we conclude from the frequency dependence of the dark and photoconductivity and from the dc and microwave Hall mobility of dark and photoexcited carriers that although barriers are present in PbS films, they are not material to the photobehavior of the films. That is, we believe that the photocarriers flow through limited but connecting channels within the films. We have not attempted to speculate on the nature of these channels or the very interesting question of their relation to film activation but have tried to restrict the

¹⁴ G. W. Mahlman, *Phys. Rev.* **103**, 1619 (1956).

¹⁵ David Dutton, *Proceedings of the Conference on Photoconductivity, Atlantic City, November 4-6, 1954*, edited by R. G. Breckenridge *et al.* (John Wiley & Sons, New York, 1956).

study as much as possible to questions of electrical structure.

ACKNOWLEDGMENTS

We wish to express our sincere thanks to Dr. R. L. Petritz for having stimulated our interest in PbS films

and for several helpful discussions throughout the course of this work. In addition, we wish to thank Dr. R. F. Brebrick of the U. S. Naval Ordnance Laboratory and Dr. Harry E. Spencer of Eastman-Kodak for generously furnishing the samples used in this investigation.

PHYSICAL REVIEW

VOLUME 120, NUMBER 6

DECEMBER 15, 1960

Microwave Faraday Effect in Silicon and Germanium*

J. K. FURDYNA

Northwestern University, Evanston, Illinois

AND

S. BROERSMA

University of Oklahoma, Norman, Oklahoma

(Received August 1, 1960; revised manuscript received September 7, 1960)

The Faraday rotation and ellipticity in a system of quasifree carriers is discussed and applied to microwave measurements on semiconductors. The theoretical expressions for these effects are analyzed with a digital computer for various ranges of the magnetic field B , the mobility μ , the conductivity σ , the frequency ω , the collision time τ and the dielectric constant of the host material. It is possible to simplify these expressions in certain limiting cases. For μB smaller than unity, the rotation and ellipticity are proportional to B . For μB larger than both unity and $\omega\tau$, they decrease as B^{-1} and B^{-3} , respectively. A maximum occurs near $\mu B = 1$ when $\omega\tau$ is small.

Rotation measurements on n - and p -type single crystals of silicon at room temperature, with resistivities from 0.5 to 40 ohm-cm, utilizing 9.6- and 35-kMc/sec radiation, are compared with the theory. Results for n -type germanium at 78°K, with μB varied up to about 6, agree with the calculated low- and high-field behavior. Faraday ellipticity measurements on n -type germanium crystals at 78°K are in qualitative agreement with the theory. In the case of small losses, the sign of the ellipticity is determined by the sign of the quantity $(4\omega\tau - \sigma/\omega\epsilon_{st})$.

A. INTRODUCTION

THE Faraday effect in a longitudinally magnetized substance can be observed as a rotation and as an elliptical polarization of an initially plane polarized wave. Here the theoretical equations will be compared with the experimental results obtained for various semiconductor samples for a broad range of conductivities.

The complex propagation constants for the left- and right-circularly polarized electric field components of a traveling electromagnetic wave (indicated by $+$ and $-$, respectively) can be written^{1,2}

$$k_{\pm}^2 \equiv (\alpha_{\pm} \mp i\beta_{\pm})^2 = \mu_0 \omega^2 (\epsilon_{\pm}' \mp i\epsilon_{\pm}''), \quad (1)$$

where μ_0 is the permeability of free space, ω the microwave angular frequency, and ϵ_{\pm}' and ϵ_{\pm}'' the real and imaginary parts of the effective dielectric constant of the medium, all in mks units.

Using the one-carrier model for semiconductors, one

can write

$$\epsilon_{\pm}' = \epsilon_{st}' - \frac{\sigma/\omega(\omega\tau \pm \mu B)}{1 + (\omega\tau \pm \mu B)^2}, \quad \epsilon_{\pm}'' = \frac{\sigma/\omega}{1 + (\omega\tau \pm \mu B)^2}, \quad (2)$$

where ϵ_{st}' is the dielectric constant of the host material, σ the dc conductivity at $B=0$, $\mu = q\tau/m^*$ the carrier mobility, τ the effective time between collisions, m^* the effective mass of the charge carriers, q the carrier charge, and B the dc magnetic field.

From Eq. (1) the propagation constants are readily found to be

$$(\alpha_{\pm}, \beta_{\pm}) = \omega(\mu_0/2)^{1/2} [(\epsilon_{\pm}'^2 + \epsilon_{\pm}''^2)^{1/2} (+, -) \epsilon_{\pm}']^{1/2}. \quad (3)$$

The angle θ through which the plane of polarization rotates as the wave progresses a distance l in the medium then is given by

$$\theta = \frac{1}{2}(\alpha_- - \alpha_+)l \text{ radians}. \quad (4)$$

Similarly, the ellipticity, i.e., the ratio of the minor to the major axis of the resulting electric field pattern, is

$$E = \tanh\left[\frac{1}{2}(\beta_- - \beta_+)l\right] \approx \frac{1}{2}(\beta_- - \beta_+)l. \quad (5)$$

On the basis of this model Rau and Caspari were able to discuss successfully their measurements on n -

* This work was supported by the National Science Foundation. (J. K. Furdyna, Thesis, Northwestern University, Evanston, Illinois, May 1960).

¹ R. R. Rau and M. E. Caspari, Phys. Rev. **100**, 632 (1955).

² M. J. Stephen and A. B. Lidiard, J. Phys. Chem. Solids **9**, 43 (1959).